Journal of Power Sources 242 (2013) 656–661

Contents lists available at SciVerse ScienceDirect

Journal of Power Sources

journal homepage: www.elsevier.com/locate/jpowsour

Low cost synthesis of $LiFePO_4$/C cathode materials with Fe_2O_3

Lifeng Cheng [a], Guoxian Liang [b], Soumia El Khakani [a], Dean D. MacNeil [a,*]

[a] Département de Chimie, Université de Montréal, Montréal, Québec H3T 1J4, Canada
[b] Clariant (Canada) Inc., 1475 Rue Marie-Victorin, St-Bruno, Québec J3V 6B7, Canada

HIGHLIGHTS

- Low cost Fe_2O_3 precursor was employed.
- A simple hydrothermal method followed by a fast calcination and carbon coating was employed.
- This method combines the advantages of both hydrothermal and solid state synthetic methods.
- This method provides enhanced electrochemical performance compared to a solid state method.
- This method is favorable to reduce the cost of large-scale synthesis of $LiFePO_4$/C.

ARTICLE INFO

Article history:
Received 28 February 2013
Received in revised form
20 May 2013
Accepted 21 May 2013
Available online 4 June 2013

Keywords:
Lithium-ion battery
Lithium iron phosphate
Ferric oxide
Hydrothermal method
Low cost
Citric acid

ABSTRACT

$LiFePO_4$/C composite materials have been synthesized from a low cost Fe_2O_3 precursor by a hydrothermal method to make $LiFePO_4$(OH) in a first step followed by a fast calcination and carbon coating. This method combines the advantages of both hydrothermal and solid state synthetic methods. The as-prepared $LiFePO_4$/C provides enhanced discharge capacity and cycling stability compared to $LiFePO_4$ synthesized using a solid state method with the same precursors. Thus, the method to be described herein is a promising option in the search to reduce the cost of large-scale synthesis of $LiFePO_4$/C for use in lithium-ion batteries, while maintaining adequate electrochemical performance.

1. Introduction

Olivine-type $LiFePO_4$ has recently become one of the most important cathode materials for Li-ion batteries because of its superior capacity retention, thermal stability, nontoxicity, safety, and potential low cost [1–4]. Despite these advantages, olivine $LiFePO_4$ has some disadvantages, such as low intrinsic electronic and ionic conductivity [5–8]. One approach to overcome this insulating nature is to coat active particles with conductive carbon [9–13], while the poor lithium-ion diffusion is addressed by synthesizing small particles with high purity [14–17].

A hydrothermal synthetic method [18–22] is a simple and low energy consumption procedure compared to solid state reactions that require high firing temperature and long dwell times [1]. Although they can be used to prepare fine particles, low temperature hydrothermal methods often result in the formation of olivine $LiFePO_4$ with poor crystallinity [23]. This decreases the electrochemical performance of the resulting $LiFePO_4$ material. In addition, most previous hydrothermal methods for $LiFePO_4$ used expensive water soluble Fe^{2+} salts as starting materials [18]. More common and less expensive ferric precursors are seldom used to synthesize $LiFePO_4$ by a hydrothermal method. Yang et al. synthesized $LiFePO_4$ using ferric precursors by a solvothermal method [24], however, a large excess of expensive LiI (LiI:Fe^{3+} = 10:1), as well as an organic solvent would increase the synthetic cost and make this process unfeasible for large-scale production.

Currently, the cost of lithium-ion batteries is still too high, with material costs accounting for up to 80% and 90% of the total costs of high power and high energy batteries, respectively [25]. Thus, there is a great potential for reducing the costs of lithium-ion batteries through development of low cost materials and material processing techniques, especially for the cathode [26,27]. Clearly, novel large

* Corresponding author. Tel.: +1 5143537054; fax: +1 5143437586.
E-mail address: dean.macneil@umontreal.ca (D.D. MacNeil).

0378-7753/$ – see front matter © 2013 Elsevier B.V. All rights reserved.
http://dx.doi.org/10.1016/j.jpowsour.2013.05.096

scale/low cost synthetic methods using low cost raw materials need to be developed.

In this work, we have employed a low cost ferric oxide (Fe_2O_3) and LiH_2PO_4 as precursor materials to prepare low cost electrochemically active $LiFePO_4$/C in two steps. In the first step, $LiFePO_4$(OH) (tavorite) was obtained by a hydrothermal method using citric acid as a chelating agent. β-lactose was then mixed with the $LiFePO_4$(OH) particles and the mixture was heated for a short period under a N_2 atmosphere to form $LiFePO_4$/C. The simultaneous realization of a carbon coating and $LiFePO_4$(OH) reduction greatly improved the crystallinity, conductivity and thus the electrochemical performance of the resulting $LiFePO_4$ material.

2. Experimental

2.1. Preparation of $LiFePO_4$/C nanoparticles

The preparation of $LiFePO_4$/C nanoparticles was realized in two steps following the schema shown in Fig. 1.

2.1.1. Synthesis of $LiFePO_4$(OH) precursor using a hydrothermal method

Stoichiometric amounts of LiH_2PO_4, Fe_2O_3 (25–30 nm, Sigma–Aldrich Co. LLC) and citric acid were added to 30 ml of water in a 40 ml Teflon-lined hydrothermal vessel. The vessel was purged with N_2 under sonication, sealed, and then placed inside a stainless steel autoclave. Subsequently, the autoclave was placed into an oven at 220 °C for 12 h. After cooling naturally to room temperature, the suspension was dried under continuous stirring at 80 °C. The solid sample was then analyzed by XRD and found to be mainly $LiFePO_4$(OH). For comparison purposes, a second batch of $LiFePO_4$(OH) was prepared using the above method, but in the absence of citric acid.

2.1.2. Synthesis of $LiFePO_4$/C from the as-prepared $LiFePO_4$(OH)

Heat treating $LiFePO_4$(OH) in the presence of β-lactose was performed for two purposes: a) to realize the formation of a carbon coating on the surface; and, b) the reduction of $LiFePO_4$(OH) to $LiFePO_4$. β-lactose (Sigma–Aldrich Co. LLC) with a 15% weight ratio with respect to $LiFePO_4$ was dissolved in 5 ml of distilled water and 40 ml of IPA (isopropyl alcohol). To the solution, $LiFePO_4$(OH) was added and the resulting slurry was dried at 80 °C for 3 h under vigorous stirring to remove the excess water and IPA. The powder was then calcined at 700 °C for 3 h in a tube furnace under a N_2 atmosphere to obtain $LiFePO_4$/C.

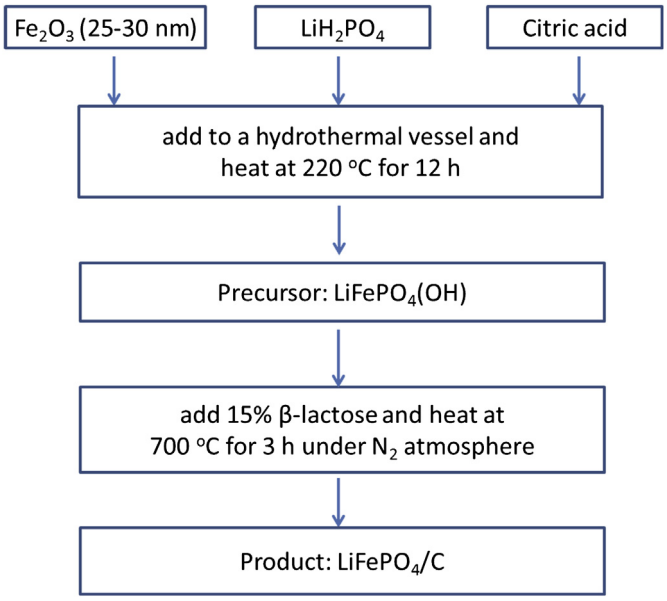

Fig. 1. Flow chart for the preparation of $LiFePO_4$/C using nano-Fe_2O_3 precursor.

2.2. Physicochemical characterizations

X-ray diffraction (XRD) was performed using a Bruker D8 Advance X-ray diffractometer equipped with Cu Kα radiation source. The particle size and morphology of each sample was examined by a Scanning Electron Microscope (Hitachi S-4300). A Fisons Instruments (SPA, model EA1108) elemental analyzer was used to determine the carbon content within the samples. The carbon content of all samples prepared as described in Section 2.1.2, was determined to be 3.8% ± 0.1%.

2.3. Electrochemical measurements

Electrochemical evaluations were performed by combining 80 wt% of the $LiFePO_4$/C powder, 10 wt% of conductive carbon (Super-P Li, Timcal) and 10 wt% polyvinylidene difluoride (PVDF, 5% in N-methylpyrrolidinone (NMP)) with an excess of NMP to form a slurry. The slurry was then deposited on a carbon coated Al foil. After drying at 90 °C overnight, electrode disks were punched and weighed for cell assembly in standard 2032 coin-cell hardware (Hohsen) using lithium metal foil as both counter and reference electrodes and a Celgard 2200 separator. The electrode area of the cathode was 1.54 cm^2 providing a $LiFePO_4$ active electrode loading of approximately 4.3 mg cm^{-2} for each sample under test. Cells were assembled in an argon-filled glove box using 1 M $LiPF_6$ in ethylene carbonate (EC)/diethyl carbonate (DEC) (2:1 by volume) as an electrolyte (UBE). Battery performance evaluations were

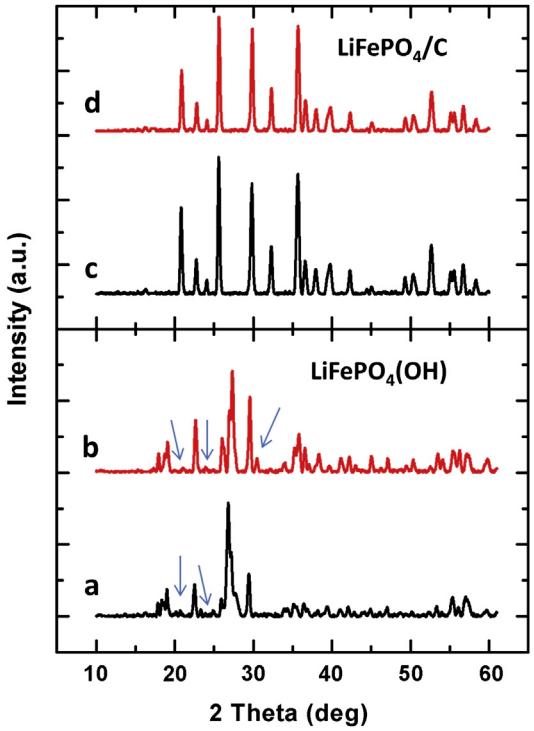

Fig. 2. XRD patterns of $LiFePO_4$(OH) precursor synthesized from commercial nano Fe_2O_3 with citric acid (a) and without citric acid (b) and corresponding $LiFePO_4$/C final product (c and d). Arrows indicate presence of impurities.

Table 1
Crystal size and color of $LiFePO_4(OH)$ and $LiFePO_4/C$ prepared with and without citric acid.

Sample	$LiFePO_4(OH)$ with citric acid	$LiFePO_4/C$ with citric acid	$LiFePO_4(OH)$ without citric acid	$LiFePO_4/C$ without citric acid
Crystal size (nm)	28.8	33.0	29.6	33.4
Color	Green	Black	Yellow	Black

performed by charging and discharging between 2.2 and 4.0 V with a current rate of 0.1 C at 30 °C using a BT-2000 electrochemical station (Arbin).

3. Results and discussion

Fig. 2a and b provides the XRD patterns of $LiFePO_4(OH)$ synthesized in the presence (a) or absence (b) of citric acid using a hydrothermal method. The major peaks can be indexed to the triclinic crystal system using the $P\bar{1}$ space group [28,29], except for several impurity peaks indicated by arrows. Citric acid, due to its strong coupling ability, has been widely used in the past as a chelating and reducing agent [21,22,30]. As shown in Table 1, the color of $LiFePO_4(OH)$ prepared with citric acid is green, while $LiFePO_4(OH)$ prepared without citric acid is yellow. The green color implies that there exists a small amount of a Fe^{2+} compound, likely the impurity seen in Fig. 2a. Moreover, there is no obvious reduction in particle size with the addition of citric acid as calculated by the Scherrer formula (Table 1) [31,32]. As mentioned in the Experimental section, the solid Fe_2O_3 precursor has a nanoscale particle size of 25–30 nm, thus, during the hydrothermal reaction, the particle size of the resulting products is not affected even in the presence of the chelating agent or surfactant. In stark comparison, a hydrothermal reaction using dissolved precursors requires a chelating agent or surfactant to be added to the solution such that the nucleation and Ostwald ripening processes can be controlled and a product with a fine particle size can be obtained.

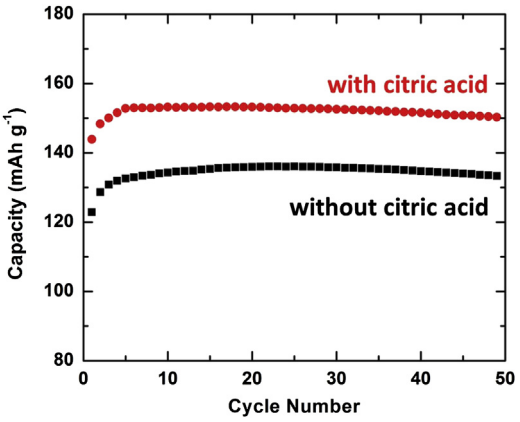

Fig. 4. Specific discharge capacity of batteries using $LiFePO_4/C$ obtained from the $LiFePO_4$ (OH) precursor synthesized without (black) and with (red) citric acid. (For interpretation of the references to color in this figure legend, the reader is referred to the web version of this article.)

Fig. 2c and d shows the XRD patterns of $LiFePO_4/C$ obtained from heating $LiFePO_4(OH)$ at 700 °C in the presence of 15% β-lactose under a N_2 atmosphere. During the heat treatment, carbon is generated from the pyrolysis of β-lactose and dispersed uniformly on the surface of $LiFePO_4(OH)$. The pyrolysis produces a strong reductive atmosphere for the resulting reduction of Fe^{3+} to Fe^{2+} and an in situ homogenous coating of carbon on the surface of the freshly formed $LiFePO_4$ particles. As seen from the XRD patterns, the in situ synthesis can produce $LiFePO_4/C$ composite materials with high crystallinity and without impurity phases such as Fe_2O_3 and $Li_3Fe_2(PO_4)_3$ that often exist in $LiFePO_4$ products prepared by conventional solid state methods [33,34]. In our case, we cannot identify any diffraction peaks resulting from carbon in the XRD pattern. The carbon likely exists in the form of an amorphous or a low-crystalline product on the surface of the $LiFePO_4$ sample. Another advantage of this in situ coating process is that the deposited carbon impedes the grain growth of $LiFePO_4$ at high

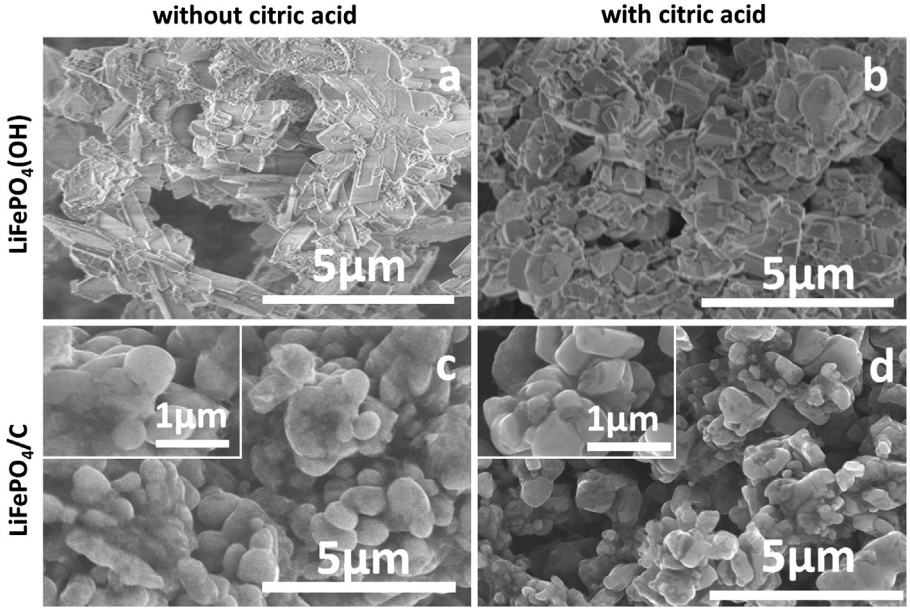

Fig. 3. SEM images of $LiFePO_4$ (OH) precursor synthesized from commercial nano Fe_2O_3 without citric acid (a) and with citric acid (b) and corresponding $LiFePO_4/C$ final product (c and d).

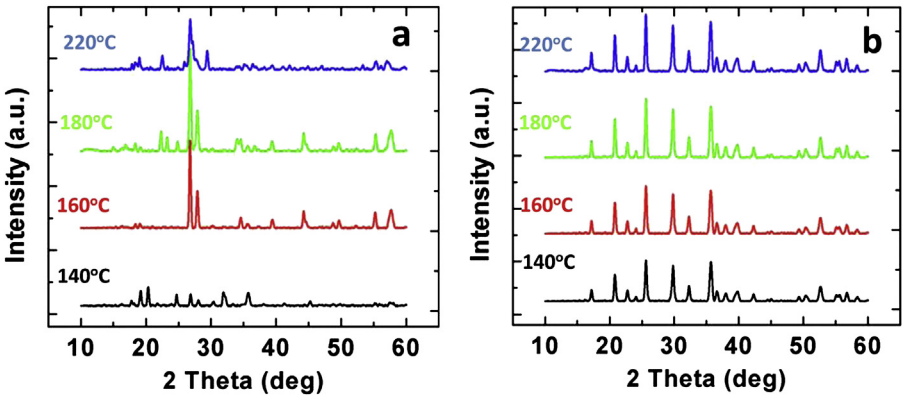

Fig. 5. (a) XRD patterns of precursors synthesized from commercial nano Fe_2O_3 at the indicated hydrothermal temperature (a) and corresponding $LiFePO_4$/C final product in (b).

temperature, thus limiting its size to that of the $LiFePO_4OH$ precursor (Table 1).

Fig. 3 shows the SEM images of the as-synthesized $LiFePO_4(OH)$ (Fig. 3a and b) and corresponding $LiFePO_4$/C (Fig. 3c and d). As shown in Fig. 3b, $LiFePO_4(OH)$ synthesized by the hydrothermal method with citric acid exhibits a uniform particle size distribution with an average particle size of ~0.7 μm. In contrast, for $LiFePO_4(OH)$ (Fig. 3a) synthesized without citric acid addition, there exists an agglomeration of particles and a larger particle size distribution in the sample (from the nanoscale to the microscale).

There is no obvious change in crystallite size with the addition of citric acid, which is confirmed by the SEM images shown in Fig. 3. However, the addition of citric acid induces a more homogeneous particle distribution within the sample. This is due to the chelating nature of citric acid with iron oxide, preventing the aggregation of iron oxide and thus $LiFePO_4(OH)$. The morphology of the carbon coated $LiFePO_4$ final product is shown in Fig. 3c and d. As seen from SEM images, there is no obvious change in particle size after heat treatment at 700 °C during the in situ carbon deposition, which is in agreement with the XRD results. In addition, $LiFePO_4$/C prepared with citric acid shows more uniform particle size distribution than that prepared without citric acid, as seen from the insert in Fig. 3c and d. The carbon content in both $LiFePO_4$/C samples is ~4 wt%.

The electrochemical properties of $LiFePO_4$/C samples synthesized with and without citric acid during the initial hydrothermal treatment are shown in Fig. 4. For both samples, there is an increase in capacity during the first several cycles due to the activation of electrode material that is often observed for carbon coated $LiFePO_4$ [35–37]. This phenomenon has been discussed in detail in the literature [38,39] and can be attributed to a slow penetration of electrolyte into the interior of the agglomerated particles. In addition, the formation of cracks within the amorphous carbon layer on $LiFePO_4$ results in a progressively increasing active surface area during the electrochemical reaction, leading to an increase in observable electrode capacity. $LiFePO_4$/C synthesized in the absence of citric acid has a much lower specific discharge capacity (~130 mAh g^{-1} at 0.1 C) than in its presence. We believe this is due to the presence of large particles which cannot be fully utilized during the electrochemical reaction, giving rise to transport limitations for both lithium ions and electrons resulting in capacity loss [40,41]. A discharge capacity of 153 mAh g^{-1} at 0.1 C is obtained for the $LiFePO_4$/C prepared using citric acid in the reaction medium. This sample maintains high capacity even after 50 cycles (98% capacity retention), due to its high purity, small/uniform particle size, uniform carbon coating and good crystallinity.

We further optimized the initial hydrothermal treatment by varying the reaction temperature to obtain a high performing $LiFePO_4$/C final product. Various hydrothermal temperatures (such as 140 °C, 160 °C, 180 °C and 220 °C) were explored for the preparation of $LiFePO_4(OH)$. As shown in Fig. 5a, there is a mixture of complex products when the chosen hydrothermal temperature is below 220 °C. Moreover, the samples are gel like and difficult to process for post heat treatment. After heating these precursors at 700 °C under an N_2 atmosphere, all of them are transformed to carbon coated $LiFePO_4$, as shown in Fig. 5b. All $LiFePO_4$/C materials are pure and well crystallized and their electrochemical performances are shown in Fig. 6. Clearly, their discharge capacity increases with increasing hydrothermal synthetic temperature. This is attributed to the higher crystallinity within the samples resulting from a higher hydrothermal reaction temperature.

For calcination, a temperature of 700 °C was chosen to limit particle growth and agglomeration, as well as to obtain enough carbonization to produce an electronically conductive carbon coating [17,42]. In previous reports, low cost Fe^{3+} precursors have been used as a starting material but a long dwell time (>10 h) under the protection of an inert (N_2, or Ar) or reductive gas, such as N_2 (or Ar) and H_2, was required [21,43]. In our experiments, post heat treatment was performed for only 3 h under N_2, which may reduce the synthetic cost during large-scale implementation.

Currently, solid state reactions are considered as a suitable method for the commercial production of $LiFePO_4$. Carbon coated $LiFePO_4$ can be synthesized using LiH_2PO_4, Fe_2O_3 and carbon as raw materials by a carbothermal reduction method (CTR) [43–46], which is simple and provides low cost. However, the high firing

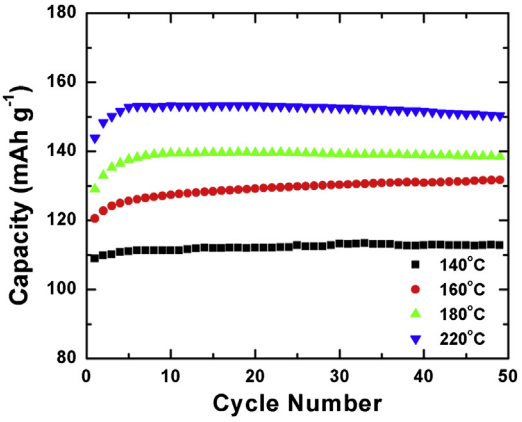

Fig. 6. Specific discharge capacity of batteries using $LiFePO_4$/C obtained from $LiFePO_4(OH)$ precursors synthesized at the indicated hydrothermal temperature.

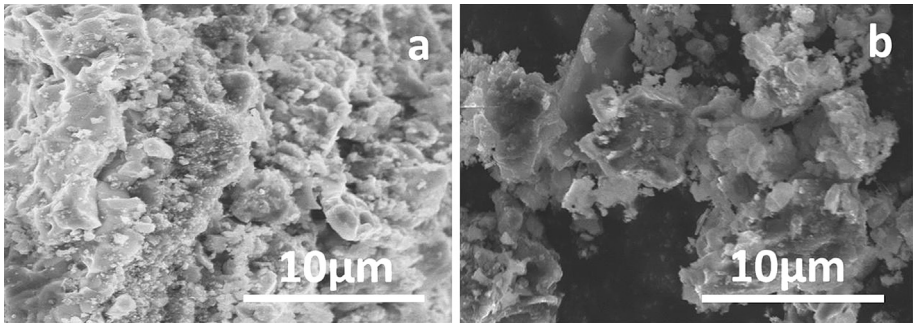

Fig. 7. SEM images of $LiFePO_4$/C obtained with commercial nano $LiFePO_4$ prepared by a solid state method at 700 °C for 3 h (a) and 10 h (b).

temperatures and long reaction times utilized in CTR methods leads to a product with large particles and poor particle size distribution [44].

In this work, for comparison purpose, we also synthesized $LiFePO_4$/C using a CTR method with the same nanosize Fe_2O_3 precursors used in Section 2.1.1. Two heat treatment times (3 and 10 h) were chosen such that we could compare methods and ensure the complete reduction of Fe^{3+}. After heat treatment, both products contain a small amount of impurity identified within the XRD patterns (not shown here) and the particles tended to aggregate due to the high calcination temperatures (visible in the SEM image shown in Fig. 7). The particle agglomeration is not favorable for the diffusion of lithium ions due to the longer pathway for migration and this leads to poor electrochemical performance (not shown here). This demonstrates the advantages of our experiments: in that, the hydrothermal reaction leads to a small and uniform particle size distribution, while the subsequent heat treatment induces high crystallinity and the complete reduction of Fe^{3+} to Fe^{2+}.

In the above experiments, we used commercial nano Fe_2O_3 as a precursor for the synthesis of $LiFePO_4$. This nano Fe_2O_3 could be replaced with low cost micron sized iron oxide to further simplify large-scale production. Thus, Fe_2O_3 powders (particle size ~ 5 μm, 99% purity) were milled in water with a planetary ball mill to obtain Fe_2O_3 in nanoscale dimensions (~200 nm in diameter). This milled Fe_2O_3 was used as the precursor for the preparation of $LiFePO_4$/C under the same conditions as described in Section 2.1. Fig. 8a shows the SEM images of the milled Fe_2O_3. It has a particle size of ca. 200 nm and uniform size distribution. Fig. 8b shows the morphology of $LiFePO_4$/C prepared with the milled Fe_2O_3, which is similar to that shown in Fig. 3d using the commercial nano Fe_2O_3. As shown in Fig. 8c, the specific discharge capacity of the as-prepared $LiFePO_4$/C is ~140 mAh g^{-1} which is much improved compared to that synthesized by the solid state method and similar in performance to that synthesized with the nano-Fe_2O_3 precursor. The results demonstrate that our method can be used as a low cost method for implementation into a large-scale production method

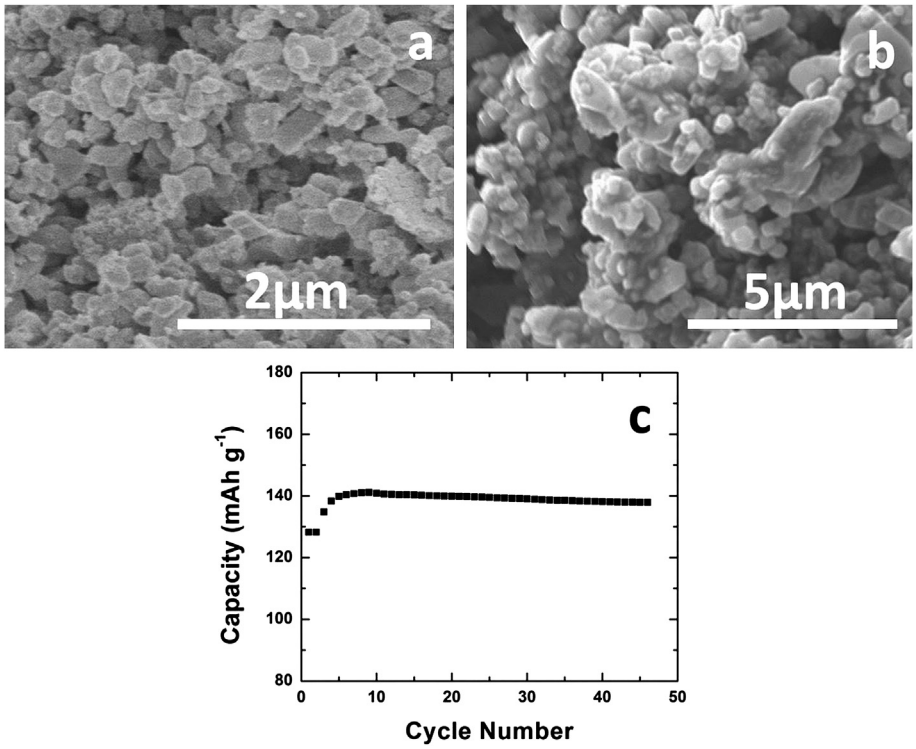

Fig. 8. (a) SEM image of commercial Fe_2O_3 precursor after planetary milling treatment. SEM image (b) and battery performance (c) of $LiFePO_4$/C synthesized with a hydrothermal method followed by post heat treatment at 700 °C using (a) as a precursor.

for $LiFePO_4$/C and eventual application within lithium-ion batteries. Another important aspect of our procedure is that we have eliminated the need to add additional lithium salts during hydrothermal synthesis. Traditional hydrothermal techniques use an excess of lithium salt ($\sim 3\times$) in their procedures and this significantly increases the costs for large-scale syntheses due to waste water treatment and precursor salt selection.

4. Conclusions

$LiFePO_4$/C composite materials have been synthesized with nano Fe_2O_3 as a precursor using a modified hydrothermal method. Our two-step method combined the advantages of both hydrothermal and solid state methods. In the first step, a $LiFePO_4$(OH) precursor with small particle size and uniform size distribution was prepared by a hydrothermal method. The heat treatment in the second step leads to the simultaneous realization of carbon coating and $LiFePO_4$(OH) reduction, producing $LiFePO_4$/C with high purity, crystallinity, specific discharge capacity and cycle stability compared to samples synthesized with the same precursors using a solid state method. Whether commercial nano Fe_2O_3 or a milled micron sized Fe_2O_3 was used as a precursor, the final $LiFePO_4$/C product exhibited excellent battery performance. Our modified hydrothermal method combined with less expensive Fe_2O_3 precursors can greatly reduce synthetic costs for $LiFePO_4$ and it is thus very promising for the large-scale synthesis of $LiFePO_4$/C cathode materials for lithium-ion batteries.

Acknowledgements

The authors thank NSERC and Clariant (Canada) Inc. (former Phostech Lithium Inc.) for funding this work under the auspices of the Industrial Research Chair program.

References

[1] A.K. Padhi, K.S. Nanjundaswamy, J.B. Goodenough, J. Electrochem. Soc. 144 (1997) 1188.
[2] A.K. Padhi, K.S. Nanjundaswamy, C. Masquelier, S. Okada, J.B. Goodenough, J. Electrochem. Soc. 144 (1997) 1609.
[3] J.M. Tarascon, M. Armand, Nature 414 (2001) 359.
[4] M.S. Whittingham, Chem. Rev. 104 (2004) 4271.
[5] M.S. Islam, D.J. Driscoll, C.A.J. Fisher, P.R. Slater, Chem. Mater. 17 (2005) 5085.
[6] D. Morgan, A. Van der Ven, G. Ceder, Electrochem. Solid-State Lett. 7 (2004) A30.
[7] C.W. Kim, J.S. Park, K.S. Lee, J. Power Sources 163 (2006) 144.
[8] S.-Y. Chung, J.T. Bloking, Y.-M. Chiang, Nat. Mater. 1 (2002) 123.
[9] Y.-D. Cho, G.T.-K. Fey, H.-M. Kao, J. Power Sources 189 (2009) 256.
[10] N. Ravet, J.B. Goodenough, S. Besner, M. Simoneau, P. Hovington, M. Armand, in: The 196th Meeting of the Electrochemical Society, Honolulu, HI, October 17–22 (1999).
[11] J.D. Wilcox, M.M. Doeff, M. Marcinek, R. Kostecki, J. Electrochem. Soc. 154 (2007) A389.
[12] A. Vu, A. Stein, Chem. Mater. 23 (2011) 3237.
[13] M.M. Doeff, J.D. Wilcox, R. Kostecki, G. Lau, J. Power Sources 163 (2006) 180.
[14] M. Gaberscek, R. Dominko, J. Jamnik, Electrochem. Commun. 9 (2007) 2778.
[15] Y. Wang, Y. Wang, E. Hosono, K. Wang, H. Zhou, Angew. Chem. Int. Ed. 47 (2008) 7461.
[16] B. Kang, G. Ceder, Nature 458 (2009) 190.
[17] A. Yamada, S.C. Chung, K. Hinokuma, J. Electrochem. Soc. 148 (2001) A224.
[18] J.J. Chen, M.S. Whittingham, Electrochem. Commun. 8 (2006) 855.
[19] S. Yang, P.Y. Zavalij, M. Stanley Whittingham, Electrochem. Commun. 3 (2001) 505.
[20] B. Ellis, W.H. Kan, W.R.M. Makahnouk, L.F. Nazar, J. Mater. Chem. 17 (2007) 3248.
[21] J. Qian, M. Zhou, Y. Cao, X. Ai, H. Yang, J. Phys. Chem. C 114 3477.
[22] Z. Lu, H. Chen, R. Robert, B.Y.X. Zhu, J. Deng, L. Wu, C.Y. Chung, C.P. Grey, Chem. Mater. 23 (2011) 2848.
[23] N.J. Yun, H.-W. Ha, K.H. Jeong, H.-Y. Park, K. Kim, J. Power Sources 160 (2006) 1361.
[24] H. Yang, X.-L. Wu, M.-H. Cao, Y.-G. Guo, J. Phys. Chem. C 113 (2009) 3345.
[25] J. Li, C. Daniel, D. Wood, J. Power Sources 196 (2011) 2452.
[26] J. Li, B.L. Armstrong, J. Kiggans, C. Daniel, D.L. Wood, Langmuir 28 (2012) 3783.
[27] J. Orlenius, O. Lyckfeldt, K.A. Kasvayee, P. Johander, J. Power Sources 213 (2012) 119.
[28] N. Marx, L. Croguennec, D. Carlier, A. Wattiaux, F.L. Cras, E. Suard, C. Delmas, Dalton Trans. 39 (2010) 5108.
[29] Y.K.K.E.A. Genkina, B.A. Maksimov, O.K. Mel'Nikov, Kristallografiya 29 (1984) 50.
[30] K.-F. Hsu, S.-Y. Tsay, B.-J. Hwang, J. Mater. Chem. 14 (2004) 2690.
[31] L. Cheng, Z. Zhang, W. Niu, G. Xu, L. Zhu, J. Power Sources 182 (2008) 91.
[32] Z. Zhang, J. Ge, L. Ma, J. Liao, T. Lu, W. Xing, Fuel Cells 9 (2009) 114.
[33] G. Arnold, J. Garche, R. Hemmer, S. Ströbele, C. Vogler, M. Wohlfahrt-Mehrens, J. Power Sources 119–121 (2003) 247.
[34] K.S. Park, J.T. Son, H.T. Chung, S.J. Kim, C.H. Lee, K.T. Kang, H.G. Kim, Solid State Commun. 129 (2004) 311.
[35] J. Popovic, R. Demir-Cakan, J. Tornow, M. Morcrette, D.S. Su, R. Schlögl, M. Antonietti, M.-M. Titirici, Small 7 (2011) 1127.
[36] L. Wang, G.C. Liang, X.Q. Ou, X.K. Zhi, J.P. Zhang, J.Y. Cui, J. Power Sources 189 (2009) 423.
[37] X.-L. Wu, L.-Y. Jiang, F.-F. Cao, Y.-G. Guo, L.-J. Wan, Adv. Mater. 21 (2009) 2710.
[38] R. Dominko, M. Bele, M. Gaberscek, M. Remskar, D. Hanzel, J.M. Goupil, S. Pejovnik, J. Jamnik, J. Power Sources 153 (2006) 274.
[39] R. Dominko, J.M. Goupil, M. Bele, M. Gaberscek, M. Remskar, D. Hanzel, J. Jamnik, J. Electrochem. Soc. 152 (2005) A858.
[40] C. Fongy, S. Jouanneau, D. Guyomard, J.C. Badot, B. Lestriez, J. Electrochem. Soc. 157 (2010) A1347.
[41] J. Li, B.L. Armstrong, J. Kiggans, C. Daniel, D.L. Wood, J. Electrochem. Soc. 160 (2013) A201.
[42] S.-H. Wu, K.-M. Hsiao, W.-R. Liu, J. Power Sources 146 (2005) 550.
[43] X. Zhi, G. Liang, L. Wang, X. Ou, J. Zhang, J. Cui, J. Power Sources 189 (2009) 779.
[44] H. Liu, P. Zhang, G.C. Li, Q. Wu, Y.P. Wu, J. Solid State Electrochem. 12 (2008) 1011.
[45] C.W. Kim, M.H. Lee, W.T. Jeong, K.S. Lee, J. Power Sources 146 (2005) 534.
[46] H.-p. Liu, Z.-x. Wang, X.-h. Li, H.-j. Guo, W.-j. Peng, Y.-h. Zhang, Q.-y. Hu, J. Power Sources 184 (2008) 469.